Supporting Information for

ORIGNAL ARTICLE

Herbal formula BWBDS alleviates polymicrobial sepsis-induced liver injury via increasing the gut microbiota *Lactobacillus johnsonii* and regulating macrophage anti-inflammatory activity in mice

Xiaoqing Fan[a†], Chutian Mai[a†], Ling Zuo[b†], Jumin Huang[a], Chun Xie[c], Zebo Jiang[d], Runze Li[e] Xiaojun Yao[a], Xingxing Fan[a], Qibiao Wu[a], Peiyu Yan[a], Liang Liu[e], Jianxin Chen[b*], Ying Xie[e*] and Elaine Lai-Han Leung[c, f*]

[a] *Dr. Neher's Biophysics Laboratory for Innovative Drug Discovery, State Key Laboratory of Quality Research in Chinese Medicine, Macau University of Science and Technology, Taipa, Macau 999078, China*

[b]*Beijing University of Chinese Medicine, Beisanhuan East Road, Beijing 100029, China*

[c]*Cancer Center, Faculty of Health Science, University of Macau, Macau (SAR), China. MOE Frontiers Science Center for Precision Oncology, University of Macau, Macau (SAR), China*

[d] *Guangdong Provincial Key Laboratory of Biomedical Imaging and Guangdong Provincial Engineering Research Center of Molecular Imaging, The Fifth Affiliated Hospital, Sun Yat-sen University, Zhuhai 519000, Guangdong Province, China*

[e]*State Key Laboratory of Dampness Syndrome of Chinese Medicine, The Second Affiliated Hospital of Guangzhou University of Chinese Medicine (Guangdong Provincial Hospital of Chinese Medicine), Guangzhou 510120, Guangdong, China*

[f] *Zhuhai Hospital of Traditional Chinese and Western Medicine, Zhuhai 519020, Guangdong, China*

[*]Corresponding author.

E-mail addresses: lhleung@um.edu.com (Elaine Lai-Han Leung), leoxieying16@outlook.com (Ying Xie), cjx@bucm.edu.cn (Jianxin Chen).

[†]These authors made equal contributions to this work.

Supplementary materials and methods

Herbal formula BWBDS extraction

BWBDS is a mixture of eight herbs including *Panax ginseng C. A. Meyer* (10 g), *Lilium brownie F. E. Brown ex Miellez var. viridulum Baker* (30 g), *Polygonatum sibiricum Delar. ex Redoute* (15 g), *Lonicera japonica Thunb.* (10 g), *Hippophae rhamnoides Linn* (10 g), *Amygdalus Communis Vas* (10 g), *Platycodon grandiflorus (Jacq.) A. DC.* (10 g), and *Cortex Phelloderdri* (10 g) were weighed by the ratio of 10:30:15:10:10:10:10:10 (w/w/w/w/w/w/w/w). The herbs were pulverized and degreased in 95% ethanol at a threefold volume (v/w). The extraction was performed twice. The precipitate was extracted with hot water at thirtyfold volume (v/w) under reflux for 2 h. The extract was concentrated in a vacuum and centrifuged at 1,100 x *g* for 15 min to remove insoluble substances. The precipitate was dissolved in water and then dialyzed against distilled water. The dialysate was lyophilized to yield BWBDS.

The qualitative and quantitative analysis of BWBDS

We entrusted Beijing Qingxi Technology Research Institute to do the qualitative and quantitative analysis BWBDS. Components of BWBDS analyzed by LC/MS/MS. Compound Discover 3.2 software was used to extract characteristic peaks from Raw MASS spectrometry data. Characteristic peaks were identified by mZCloud online database and mzVault database of natural products of Traditional Chinese medicine. The screening criteria for positive results were mass deviation <5ppm, conforming isotope distribution and matching score >70 points in mzVault Best Match database.

Network pharmacology analysis

The candidate compounds of BWBDS were collected from multiple popular TCMs databases. All pharmacokinetic properties were identified from TCMSP database (https://tcmsp-e.com/). Oral bioavailability (OB) and drug likeness (DL), as crucial indicators of pharmacokinetic properties, were selected to identify BWBDS active

ingredients and the threshold was OB≥30% and DL≥0.18. All the corresponding targets of active components were acquired from TCMSP database. The official gene symbols and UniProt ID of corresponding proteins were obtained from UniProt database (https://www.Uniprot.org). Components without known targets or standard names were deleted.

"polymicrobial sepsis", "sepsis", "bacterial sepsis", "septicopyemia" and "pyemia" were the key words to gather polymicrobial sepsis-related genes from following four databases: Genecards (http://www.genecards.org), OMIM (http://omim.org/), DisGenet (https://www.disgenet.org/), TTD (http://db.idrblab.net/ttd/) and diseases (https://diseases.jensenlab.org/).

Herbs, components, disease, and target genes were imported into R 4.1.1 to build the network model of "Herb-Ingredient-Disease-Gene". Construction of protein–protein interaction (PPI) of target proteins was completed in the STRING database (http://string-db.org/, ver.11.0). The PPI network was then inputted into R4.1.1 and the top 10 genes was selected. R package digraph, ggplot2, and cluster Profiler was used for GO, KEGG analysis and data visualization.

Clinical Score

The roach back or emaciation, colon thickening, and pellet morphology were recorded during the experiment. The clinical score was calculated according to previously described scoring system[1].

Protein expression and biochemical analysis

Whole blood was withdrawn in tubes containing no anticoagulant. Blood was allowed to clot for 30 min. Solutions were centrifuged at 1,200 x *g* for 10 min and supernatants (serum) were collected. ELISA kits were used to measure interleukin (IL)-1β,

interleukin (IL)-10, interleukin (IL)-6 and tumor necrosis factor-alpha TNF-α from serum according to the manufacturer's instructions (R&D Systems, USA).

Biochemistry assay

Mice serum levels of alanine aminotransferase (ALT) and aspartate aminotransferase (AST) were measured by using commercial kits according to the manufacturer's instructions (Nanjing Jiancheng Bioengineering Institute, Nanjing, China).

Gene expression analysis

Total RNA was extracted from tissues or cells with Trizol reagent according to the manufacturer's instructions, and reverse transcription was carried out with a reverse transcription enzyme (TOYOBO) according to the manufacturer's instructions. Real-time PCR was carried out on an ABI 7500 real-time PCR system using primer sequences. Relative expression was calculated using the comparative threshold cycle (Ct) and expressed relative to control or WT (ΔΔCt method).

Histological staining

Liver, ileum, lung, and kidney tissue samples tissue was collected and fixed in 4% paraformaldehyde. Then, the samples were embedded in paraffin, 5-μm-thick sections were sliced and were stained with hematoxylin eosin (HE) for morphological examination. Liver histological damage was assessed according to previously described scoring system. The parameters for inflammation, thrombus formation and necrosis

were each graded on a scale of 0 to 4, with 0 defined as “absent” and 4 defined as “severe.” The total “histological score of liver” was expressed as the sum of the scores for each parameter, with a maximum score of 12[2]. Ileum, lung, and kidney tissue histological damage were assessed according to previously described scoring system. Ileum, lung, and kidney sections were scored on necrosis, loss of brush border, cast formation, and tubule dilatation using the scale given above, with a maximum score of 16. Lung sections were scored on alveolar congestion, hemorrhage, aggregation of neutrophils or leukocyte infiltration, and thickness of the alveolar wall using the scale given above, with a maximum score of 16. The degree of ileum and colon injury was according to changes of the intestinal mucosa necrosis, villus, glands, and lamina propria separation with a maximum score of 16. Slides were scanned and observed under a Leica optical microscope (Leica Biosystems Imaging, USA)[2].

Peritoneal macrophage collection

Injection of 4 ml of normal saline solution into the peritoneum was used for peritoneal macrophage collection, and the mice's abdomen was gently rubbed for 2 min to make the liquid ow in the abdominal cavity. The peritoneal fluid was sucked out and transferred into a centrifugal tube with a glue-head dropper. The amount of each suction was about 4~5 ml. The collected peritoneal lavage fluid (PLF) was centrifuged at 300 x *g* for 10 min and the supernatant was removed, then further flow experiment was carried out.

Polarization of peripheral blood mononuclear cells (PBMCs) derived monocytes *in vitro*

PBMCs from different group mice were isolated by Ficoll Paque density-gradient centrifugation. After washing, monocytes were isolated by Percoll density-gradient centrifugation. Monocytes were cultured in RPMI supplemented with 10% heat-inactivated FBS, penicillin 100 U/ml, streptomycin 100 mg/ml and 10 ng/ml M-CSF (Repro Tech, London, UK). After 3-4 days same amount of medium was added to the cultures. After 6-7 days, non-adherent cells were aspirated, and the adherent macrophages were incubated with indicated conditions. Macrophage differentiation was induced by culturing monocytes with IL-4 (20 ng/mL) and IL-13 (20 ng/mL) in order to obtain M2 polarized macrophages or with IFN-gamma (20 ng/mL) and LPS (100 ng/ml) for classical macrophage activation (M1) in RPMI supplemented with 10% heat-inactivated FBS, penicillin 100 U/ml, streptomycin 100 mg/ml.[3] After 24h, the cells were harvested for flow cytometry analysis.

Liver macrophages collection

For quantification of monocyte-derived macrophages in livers of mice subjected to CLP surgery, livers were collected and homogenized in Hank's buffered saline solution containing 1.49 mg/ml of collagenase type IV (Sigma-Aldrich; #C5139)[4]. The method for cell labeling and analyzed were the same as described previously (*2.3 Flow cytometry and antibodies*).

Bacterial strains

L. johnsonii (ATCC11506) freeze-dried powder (ATCC, USA) was dissolved with 0.5 ml MRS medium (HB0384-1, Qingdao Hope Bio-Technology Co., Ltd, China), then the bacteria liquid was coated on the MRS agar plate, and bacterial colonies appeared after about 24 h. Single colonies were picked into MRS medium. Bacteria strains were grown at 37°C in a Whitley A35 anaerobic workstation (Don Whitley, UK) with mixed anaerobic gas (5% carbon dioxide, 5% hydrogen, 90% nitrogen). Anaerobicity was confirmed using an anaerobic indicator (Oxoid, UK). OD600=0.6-0.7 of cultures was measured until mid-log phase after 12-16 h of growth, at which time the colony count

was detected by plate count. Frozen stocks of bacterial strains (in PBS with 20% glycerol) were prepared, stored at -80 °C for further experiments. 50 µl frozen stocks of strains were added to 5 ml MRS medium and incubated at 37 °C under anaerobic conditions for 12 h, and then used for gavage of mice. For heat inactivated-*L. johnsonii* (HI-*L. johnsonii), L. johnsonii* were harvested by centrifugation (10,000 x *g* for 20 min), washed with PBS, and heat-treated at 70°C for 30 min by a plate heat exchanger (Alfa Laval RF 372, Alfa Laval Mid Europe AG, Dietlikon, Switzerland). Heat treatment resulted in no residual CFU in the preparation. All samples were kept frozen at -80°C until use[5].

Protein expression and biochemical analysis in RAW264.7 cell *in vitro*

For the assay of cytokines, the RAW264.7 cell ($5x10^5$ cells) were stimulated with LPS (100 ng/ml; Invitrogen, CA, USA) for 4 h and 20 h in the presence or absence of different bacterial strains ($1x10^7$ CFU per well), and centrifuged at 1,200 x *g* for 10 min. In addition, the supernatant was transferred to 96-well ELISA plates, and the cytokines (IL-10, TNF-α, IL-1β, IL-6) were measured by ELISA kits according to the manufacture's protocol.

Evaluation of Systemic and Local Bacterial Burden

Blood samples were collected and spread on blood agar plate with dilutions of 1, 10, or 100 µl in 100-µl saline aliquots. Peritoneal lavage fluid (PLF) was harvested after injecting 2 ml of PBS into the peritoneum and serial dilution in sterile saline. A 100-µl aliquot of each dilution was spread on a blood agar plate. All plates were incubated at 37°C for 24–48 hours. Colonies were counted and expressed as CFU/100 µl for blood samples or CFU/ml for peritoneal lavage samples[6].

References

1. Chen G, Huang B, Fu S, Li B, Ran X, He D, et al. G Protein-Coupled Receptor 109A and Host Microbiota Modulate Intestinal Epithelial Integrity During Sepsis.

Frontiers in Immunology 2018;**9**.

2. Gong S, Yan Z, Liu Z, Niu M, Fang H, Li N, et al. Intestinal Microbiota Mediates the Susceptibility to Polymicrobial Sepsis-Induced Liver Injury by Granisetron Generation in Mice. *Hepatology* 2019;**69**:1751-67.
3. Genin M, Clement F, Fattaccioli A, Raes M, Michiels C. M1 and M2 macrophages derived from THP-1 cells differentially modulate the response of cancer cells to etoposide. *BMC Cancer* 2015;**15**:577.
4. Han YH, Onufer EJ, Huang LH, Sprung RW, Davidson WS, Czepielewski RS, et al. Enterically derived high-density lipoprotein restrains liver injury through the portal vein. *Science* 2021;**373**.
5. Lim S-M, Jang H-M, Jeong J-J, Han MJ, Kim D-H. Lactobacillus johnsonii CJLJ103 attenuates colitis and memory impairment in mice by inhibiting gut microbiota lipopolysaccharide production and NF-κB activation. *Journal of Functional Foods* 2017;**34**:359-68.
6. Huang X, Venet F, Wang YL, Lepape A, Yuan Z, Chen Y, et al. PD-1 expression by macrophages plays a pathologic role in altering microbial clearance and the innate inflammatory response to sepsis. *Proc Natl Acad Sci U S A* 2009;**106**:6303-8.

Supplementary figures

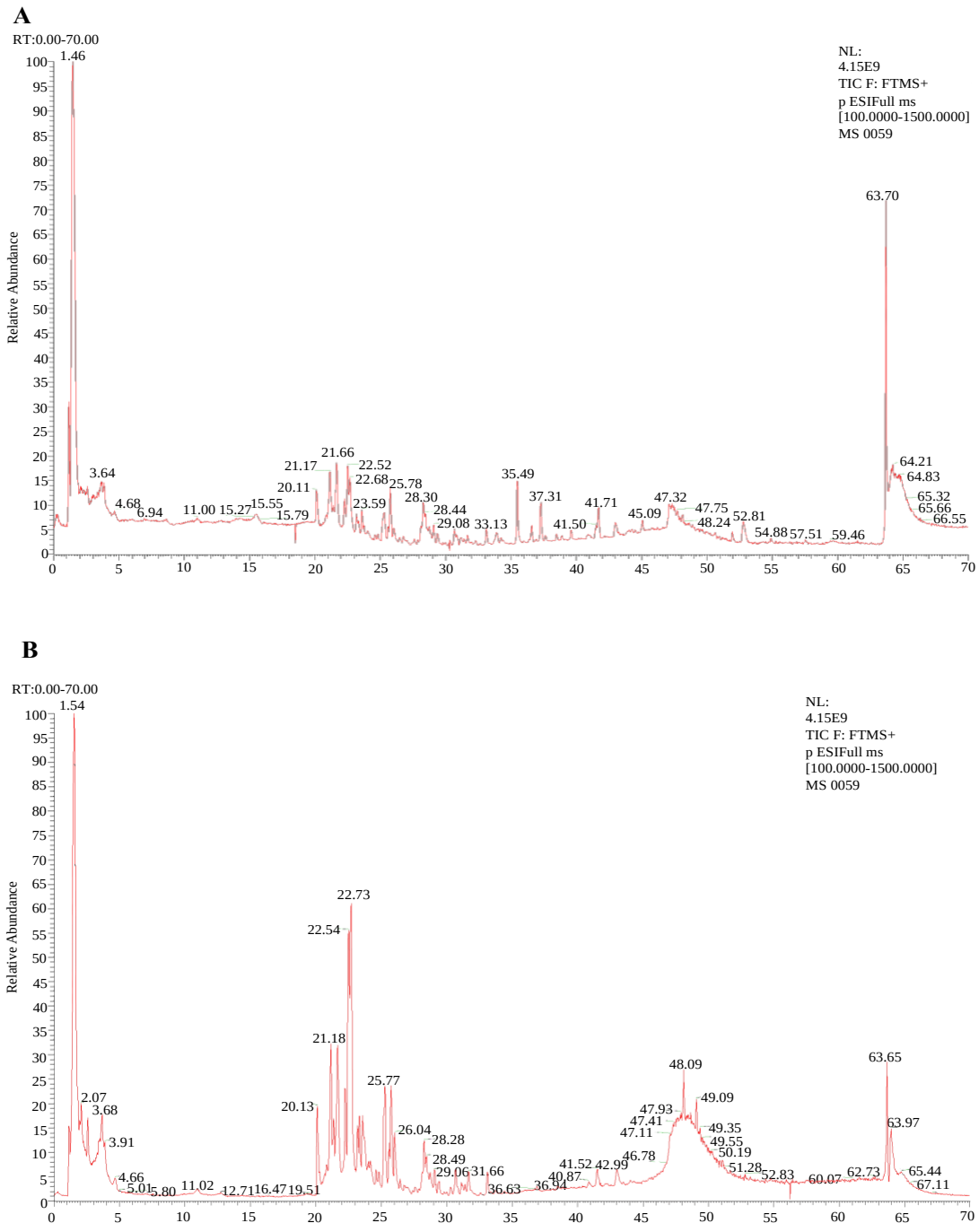

Figure S1 TTIC scans in positive and negative ion modes of BWBDS. (A) TIC diagram of sample in positive ion mode. (B) TIC diagram of sample in anion mode.

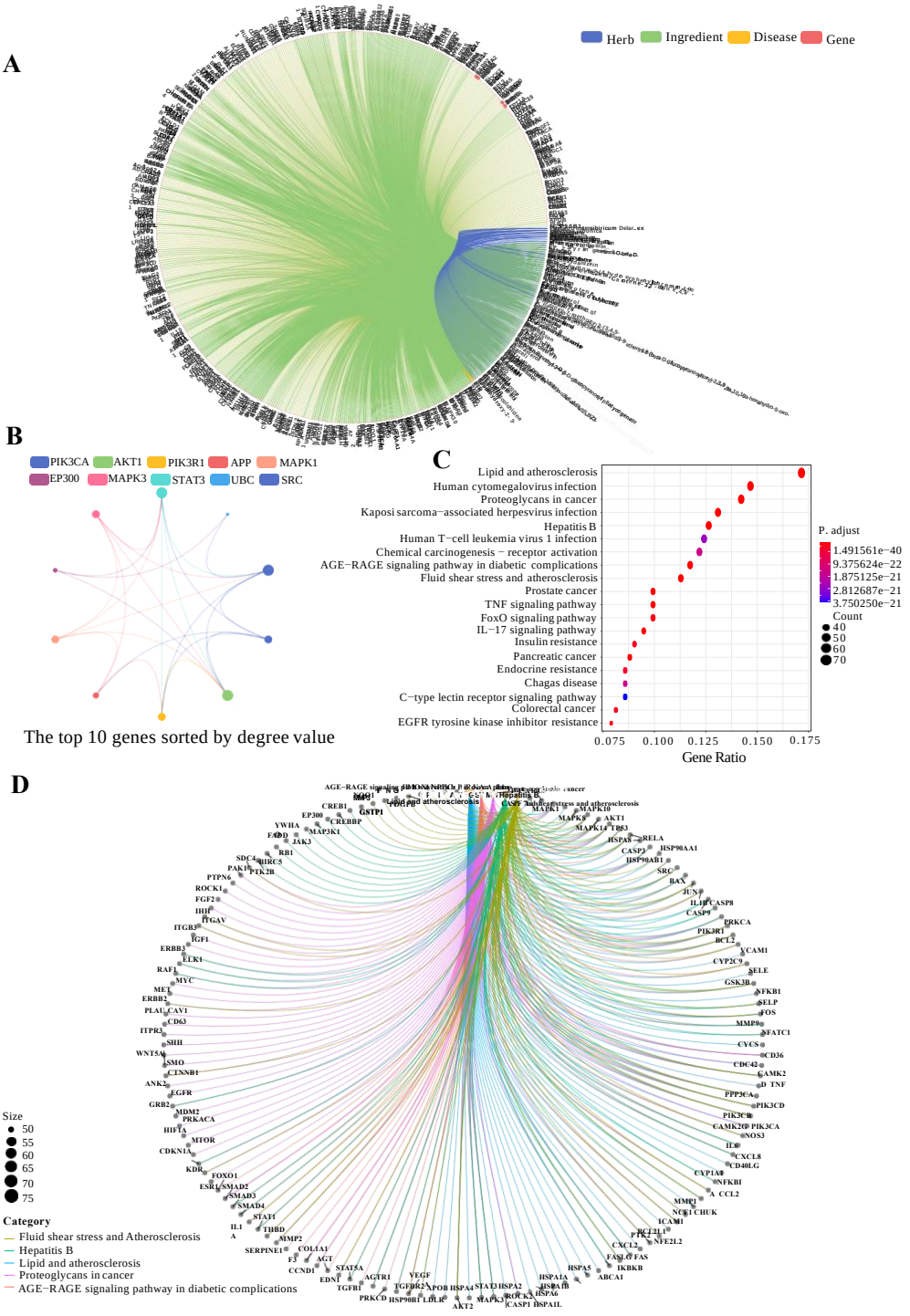

195 **Figure S2** Network pharmacology results of BWBDS. (A) "Herb-Ingredient-
196 Disease-Gene" network diagram of BWBDS. The herbs, ingredients, disease, genes,
197 and connection between them were colored. (B) The top 10 genes sorted by degree
198 value. (C) KEGG enrichment analysis results of BWBDS. (D) The top 5 genes included
199 in KEGG pathways (Sort by the number of KEGG pathways related to gene. The

greater the degree of overlap of genes, the more the same pathways involved). Lines with different colors indicate different gene-pathway relationships.

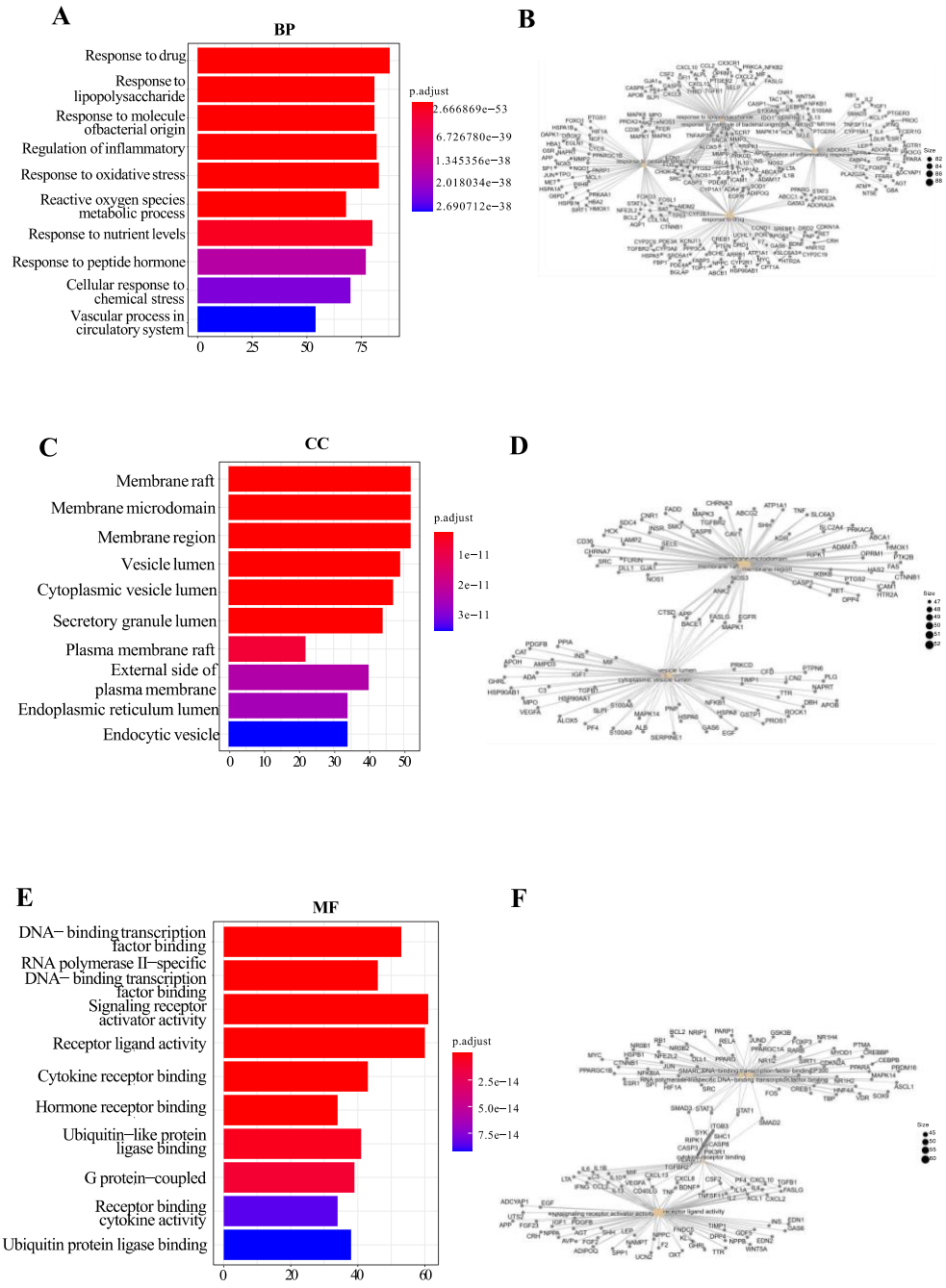

Figure S3 GO enrichment analysis results. The top 10 biological processes (A), cell components (C) and molecular functions (E) and the top 5 genes correspond to three GO terms (B, D, F). Genes were sorted by the number of GO terms related to gene. Lines with different colors indicate different gene-term relationships.

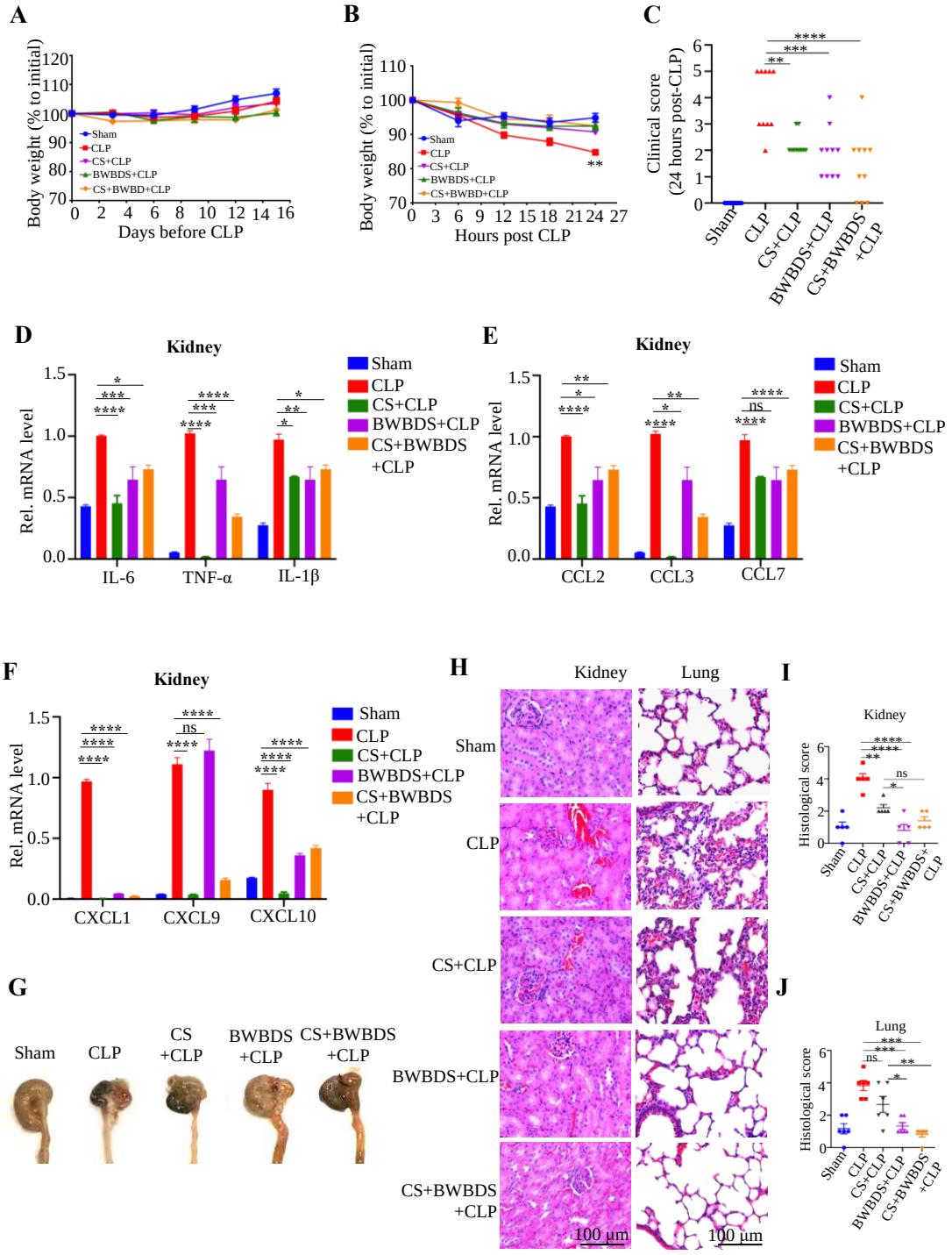

206 **Figure S4** BWBDS protects mice against sepsis-induced tissues injury. (A) Body
207 weight before CLP. (B) Body weight after CLP. (C) Clinical score. (D-F) IL-6, TNF-
208 α, IL-1β, CCL2, CCL3, CCL7, CXCL1, CXCL9, CXCL10 mRNA levels of kidneys.
209 (G) Cecum of different groups. (H-J) H&E staining (400x) and histological score of
210 kidneys and lungs. n=9-11. Scale bar=100 μm. Error bars represent the mean ± SEM.
211 Body weight curves were assessed by two-way ANOVA. The other data were

determined by one-way ANOVA. (*P<0.05, **p<0.01, ***p<0.001; ns, nonsignificant).

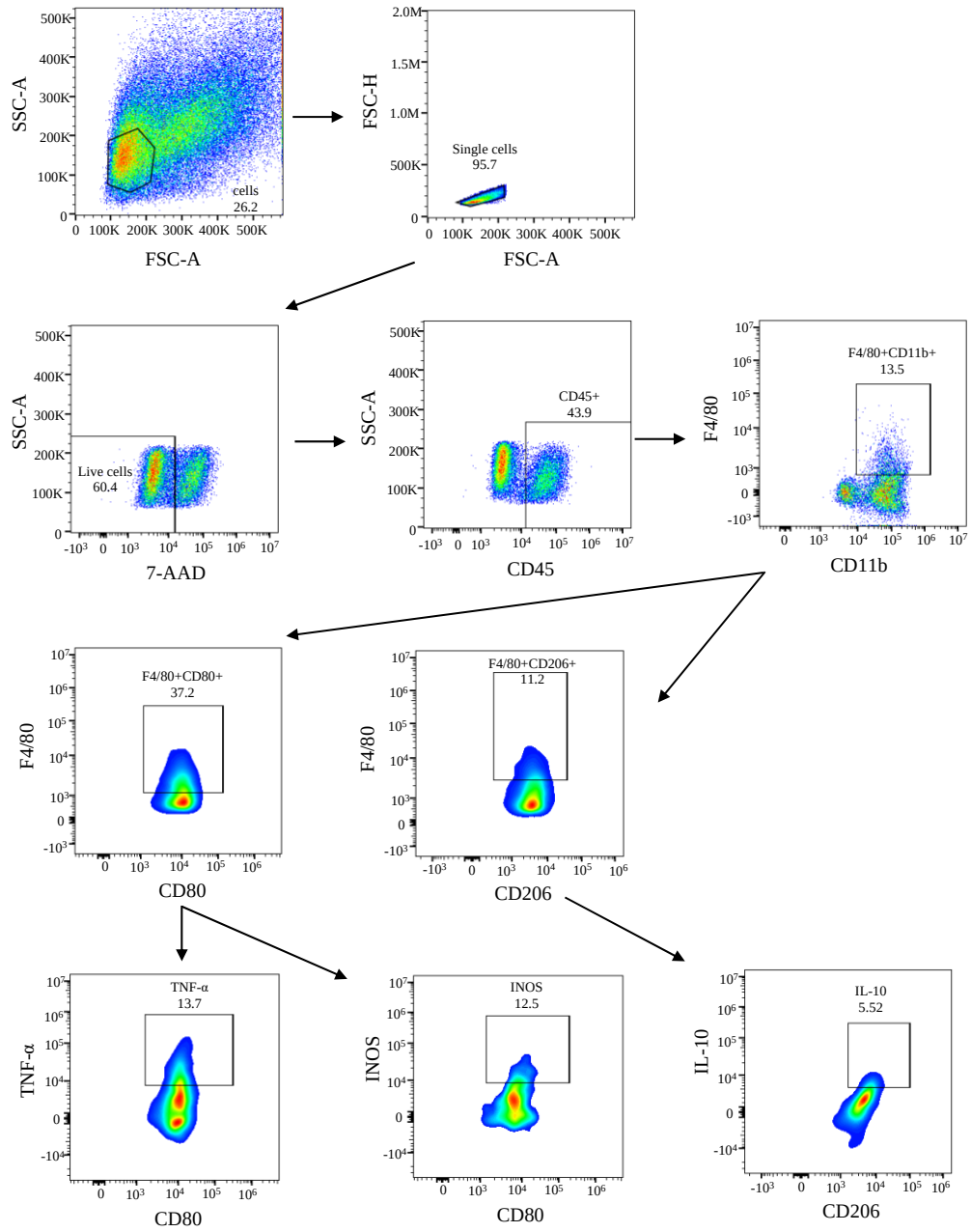

Figure S5 Flow cytometry analysis of TNF-α, iNOS among $CD80^+F4/80^+$cells and IL-10 among $CD206^+F4/80^+$ cells.

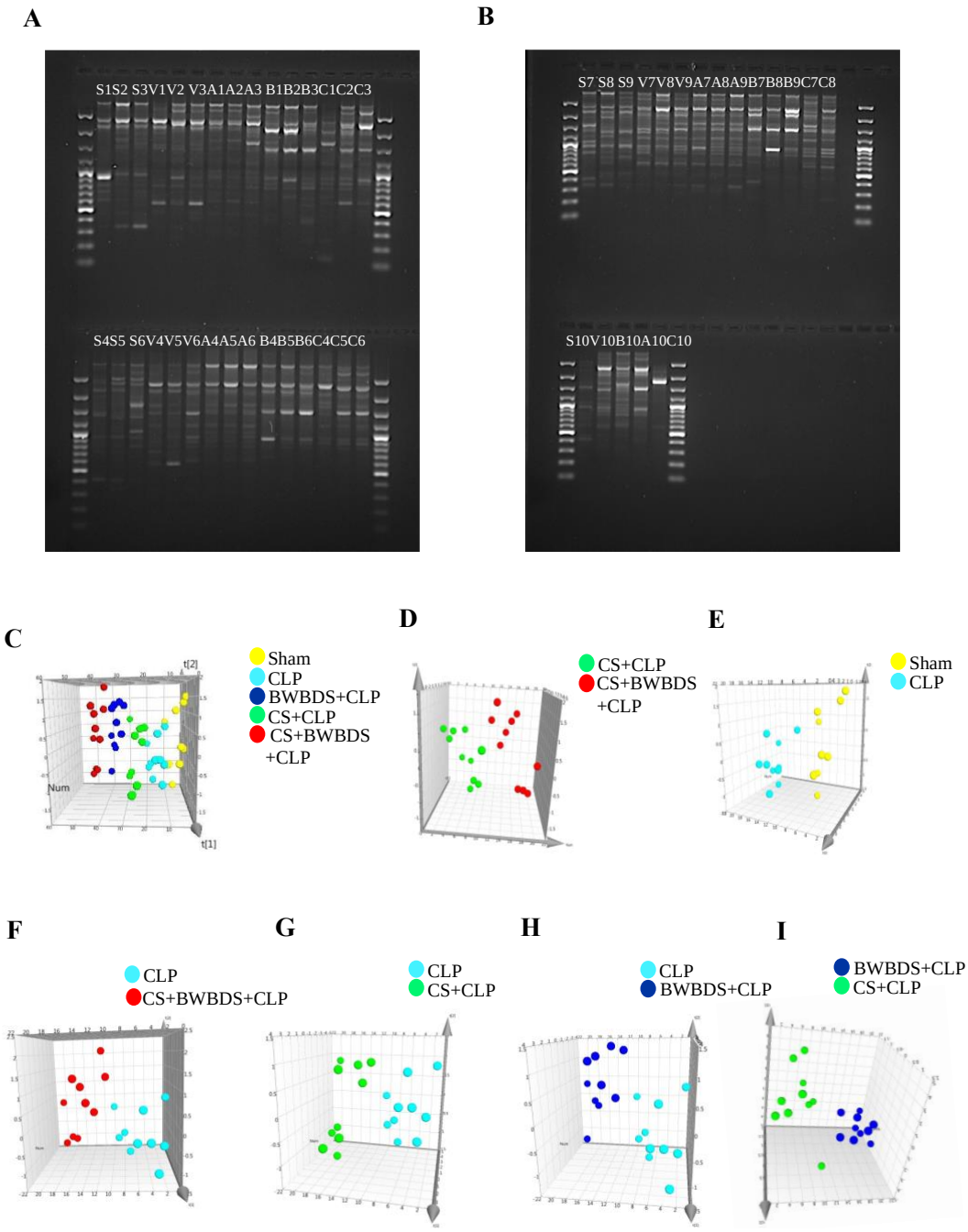

Figure S6 ERIC-PCR for differential therapy groups after CLP. (A) and (B) Representative ERIC-PCR DNA fingerprints of the fecal microbiota of individual in different therapy groups. (C-I) Scores plot of OPLS-DA model processing for CS + CLP vs. CS + BWBDS + CLP (D), Sham vs. CLP (E), CS + BWBDS + CLP vs. CLP (F), CS + CLP vs. CLP (G), BWBDS + CLP vs. CLP (H), and CS + CLP vs. BWBDS

+ CLP (I) respectively. S, sham; V, CLP; A, CS + CLP; B, BWBDS + CLP; C, CS+BWBDS+CLP.

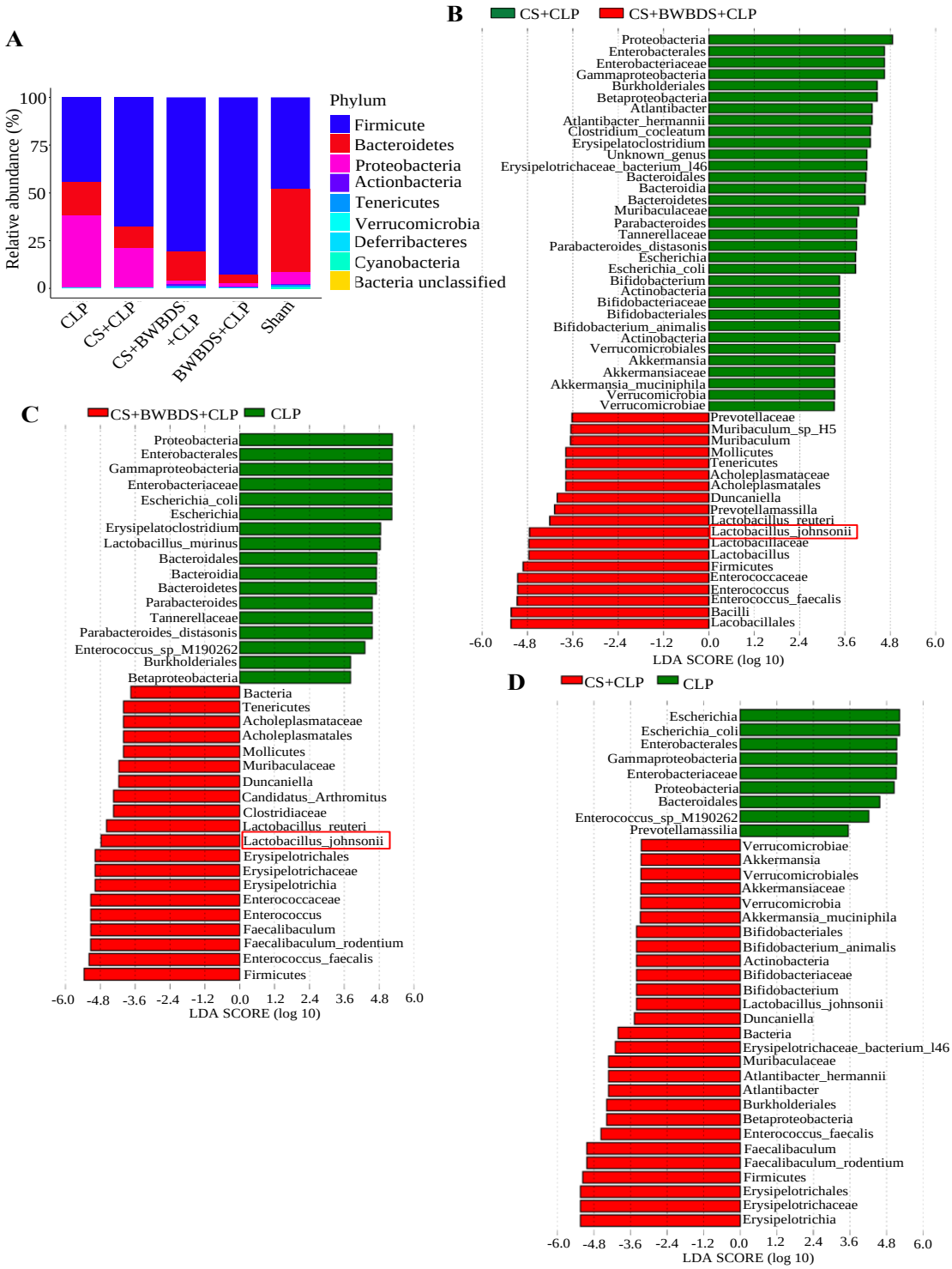

Figure S7 LEfSe analysis for differential abundant taxa after CLP from different group. (A) Relative abundance of top 10 phylum in different treatment groups. (B) LEfSe analysis between CS + CLP and CS + BWBDS + CLP group. (C) LEfSe analysis

between CS + BWBDS + CLP and CLP alone group. (D) LEfSe analysis between CS + CLP and CLP alone group. Threshold parameters were set as p=0.05 for the Mann-Whitney test and multi-class analysis=all against all. LDA score >2.0.

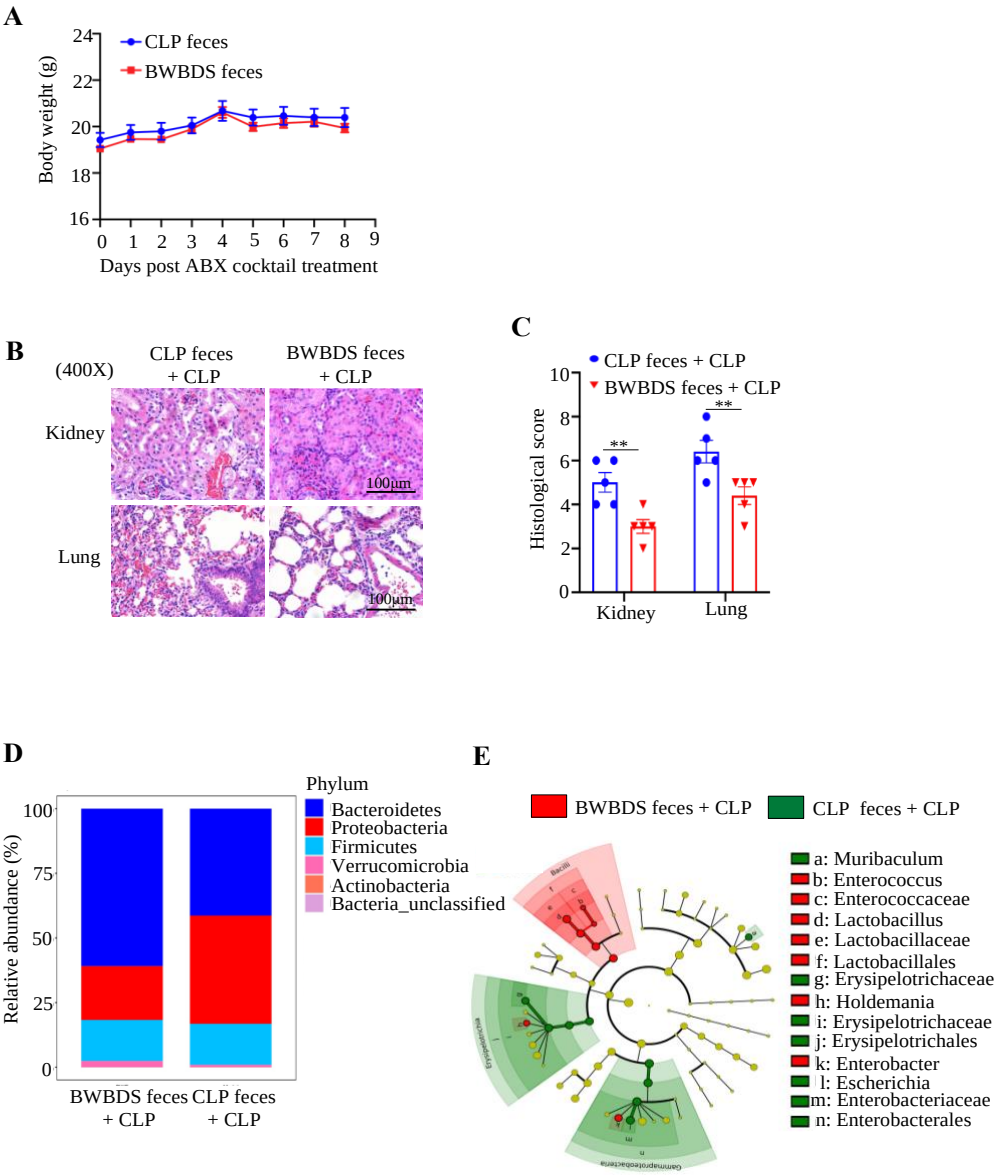

Figure S8 BWBDS feces protects mice against sepsis-induced kidney and lung tissues injury. (A) Body weight post ABX cocktail treatment. (B, C) H&E staining (400x) and histological score of kidneys and lungs. (D) Relative abundance of top 6 phylum in different treatment groups. (E) Cladogram analysis between BWBDS feces + CLP group and CLP feces + CLP group. n=5. Scale bar=100 μm. The results are expressed as the mean ± SEM. Body weight curves were assessed by two-way ANOVA. (*P<0.05, **p<0.01, ***p<0.001; ns, nonsignificant).

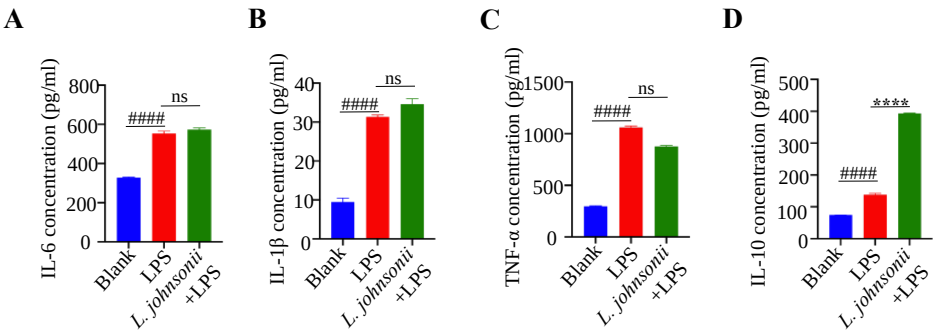

Figure S9 *L. johnsonii* enhances IL-10 levels in RAW264.7 cells upon LPS (100 ng/ml) stimulation for 24h. (A-D) IL-6, IL-1β, TNF-α and IL-10 levels in cell supernatant. n=3. Error bars represent the mean ± SEM. The data were determined by one-way ANOVA. (*P<0.05, **p<0.01, ***p<0.001; ns, nonsignificant).

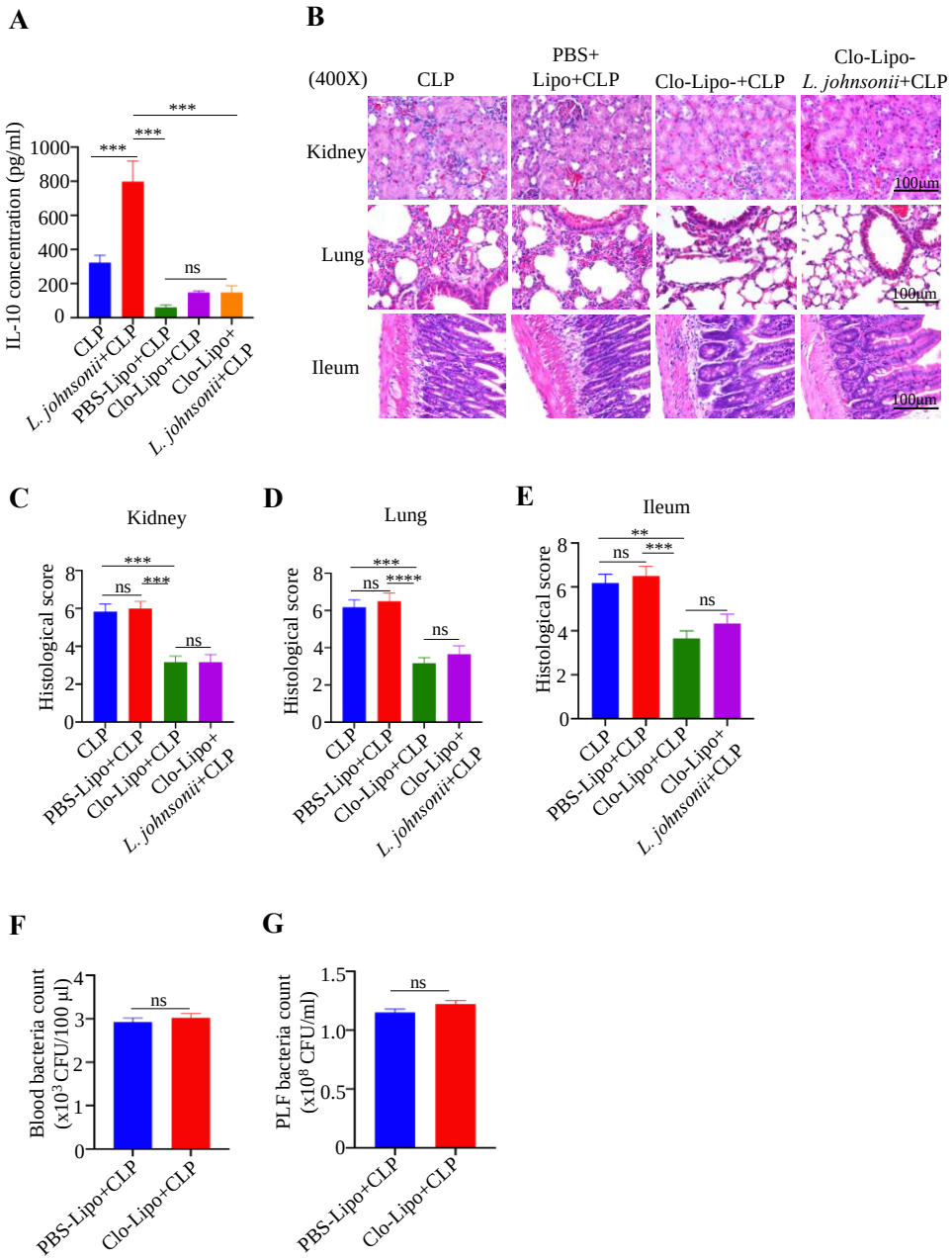

242 **Figure S10** *L. johnsonii* improves CLP-induced kidneys, lungs, and ileums tissues
243 injury depending on the participation of macrophages. (A) Serum IL-10 level. (B-E)
244 H&E staining (400x) and histological score of kidneys, lungs, and ileums. (F, G)
245 Bacteremia of blood and PLF were no different in PBS-Lipo + CLP mice and Clo-Lipo
246 + CLP mice. Bacterial counts were determined 24 h after CLP. n=5. Scale bar=100 μm.
247 The results are expressed as the mean ± SEM. (*P<0.05, **p<0.01, ***p<0.001; ns,
248 nonsignificant).

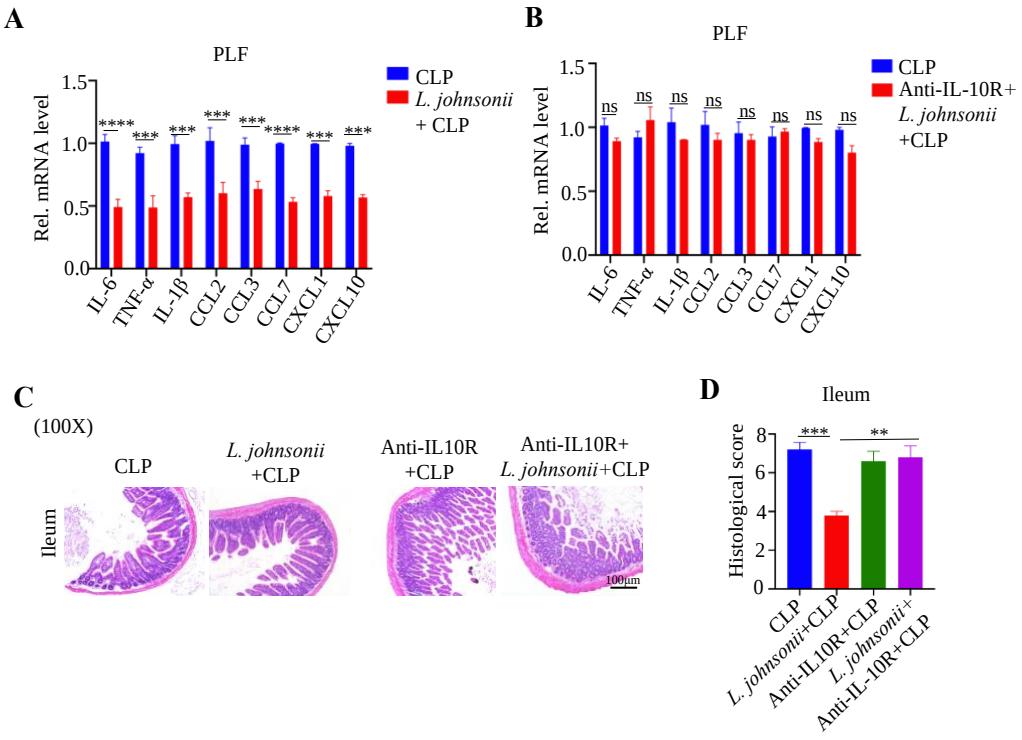

249 **Figure S11** *L. johnsonii* regulates M2 macrophages to alleviate sepsis injury. (A) IL-
250 6, TNF-α, IL-1β, CCL2, CCL3, CCL7, CXCL1, CXCL10 mRNA levels of PLF in *L.*
251 *johnsonii*-treated mice and CLP control mice. (B) IL-6, TNF-α, IL-1β, CCL2, CCL3,
252 CCL7, CXCL1, CXCL10 mRNA levels of PLF in anti-IL-10R plus *L. johnsonii*-treated
253 mice and CLP control mice. (C, D) H&E staining (400x) and histological score of
254 ileums. n=5. Scale bar=100 μm. The results are expressed as the mean ± SEM. (*P<0.05,
255 **p<0.01, ***p<0.001; ns, nonsignificant).

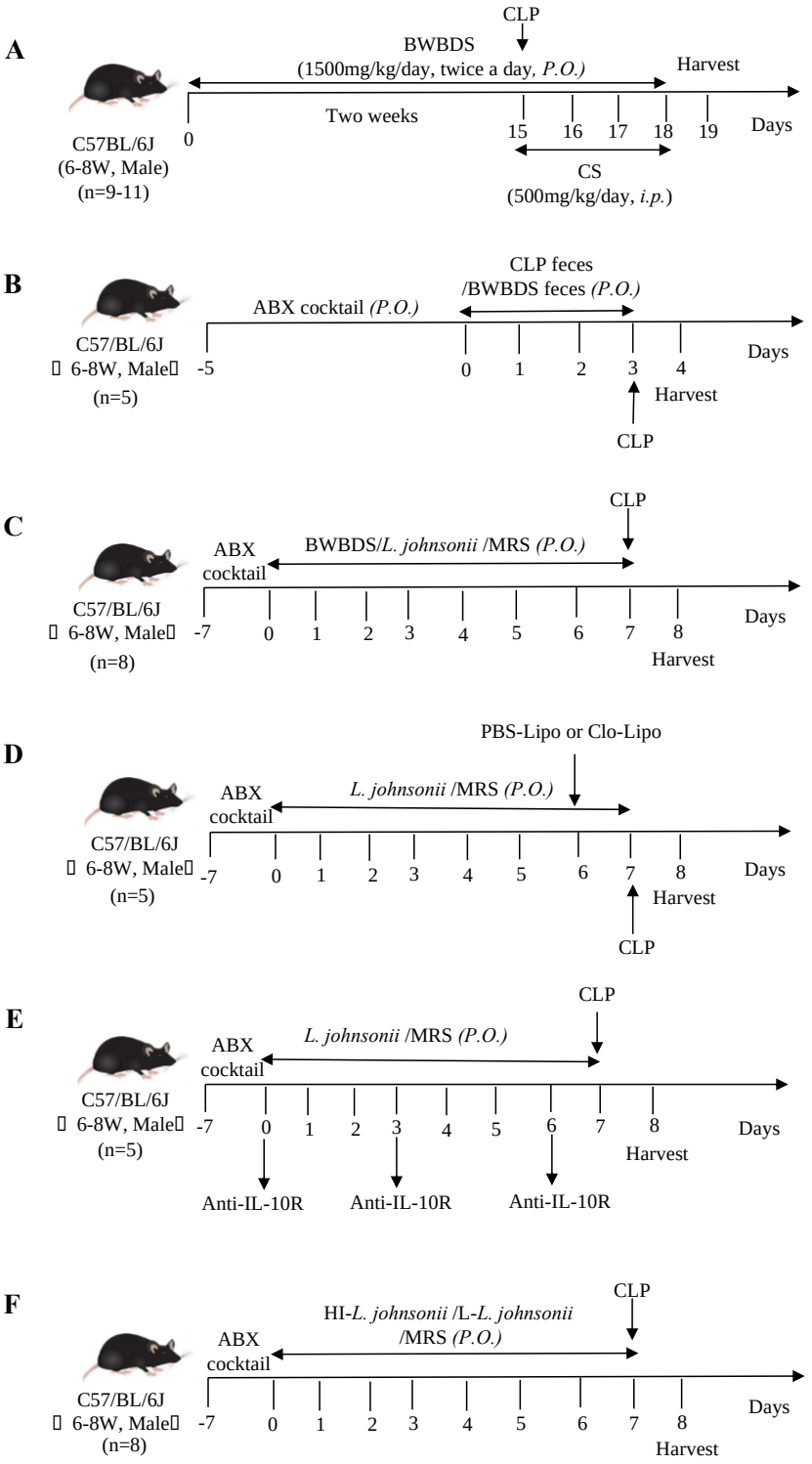

Figure S12 Experimental design. (A) BWBDS pretreatment experiment. (B) FMT experiment. (C) *L. johnsonii* pretreatment experiment. (D) Macrophage depletion experiment. (E) IL-10 depletion experiment. (F) HI-*L. johnsonii* pretreatment experiment.

Table S1 Primer sequences.

Gene	Forward primer (5'-3')	Reverse primer (5'-3')
TNF-α	CCACCACGCTCTTCTGTCTAC	AGGGTCTGGGCCATAGAACT
IL-6	TGATGCACTTGCAGAAAACA	ACCAGAGGAAATTTTCAATAGGC
IL-1β	GGTCAAAGGTTTGGAAGCAG	TGTGAAATGCCACCTTTTGA
CCL2	CCTGCTGTTCACAGTTGCC	ATTGGGATCATCTTGCTGGT
CCL3	ACCATGACACTCTGCAACCA	GTGGAATCTTCCGGCTGTAG
CCL7	CTGCTTTCAGCATCCAAGTG	TTCCTCTTGGGGATCTTTTG
CXCL1	ACCCAAACCGAAGTCATAGC	TCTCCGTTACTTGGGGACAC
CXCL10	CTCATCCTGCTGGGTCTGAG	CCTATGGCCCTCATTCTCAC
IL-10	GCTCTTACTGACTGGCATGAG	CGCAGCTCTAGGAGCATGTG
Occludin	CATTTATGATGAACAGCCCC	GGACTGTCAACTCTTTCCGC
ZO-1	GAGGGACTGTGGATGTCCTG	ATGCCAATTACCATCAAGGC
GAPDH	TGACCTCAACTACATGGTCTACA	CTTCCCATTCTCGGCCTTG

Table S2 Components of BWBDS analyzed by LC/MS/MS.

Compounds Name	RT [min]	Formula	Calc. MW	Peak area	Relative content (%)
Amygdalin	22.73	C20 H27 N O11	457.15822	7067992060	15.41
Cryptochlorogenic acid	22.56	C16 H18 O9	354.09485	4948142258	10.788
Citric acid	3.62	C6 H8 O7	192.02697	4426975372	9.652
Nobiletin	35.51	C21 H22 O8	402.13099	3076929076	6.708
Quinic acid	1.57	C7 H12 O6	192.06341	2604596076	5.679
Geniposidic acid	22.50	C16 H22 O10	374.12096	2486851971	5.422
Tangeretin	37.30	C20 H20 O7	372.12071	2215011933	4.829
Isochlorogenic acid C	26.05	C25 H24 O12	516.12634	2107429162	4.594
Secoxyloganin	23.61	C17 H24 O11	404.13171	1337998099	2.917
Isochlorogenic acid B	25.22	C25 H24 O12	516.12634	1307775618	2.851
Mannitol	1.47	C6 H14 O6	182.07893	1167807403	2.546

Verbenalin	24.06	C17 H24 O10	388.13678	939608388	2.049
3,5-Dicaffeoylquinic acid	25.62	C25 H24 O12	516.12629	652558427.4	1.423
Sucrose	2.09	C12 H22 O11	342.11602	550312123	1.2
2-Pyrrolidinecarboxylic acid	1.57	C5 H9 N O2	115.06327	538657740.1	1.174
Manninotriose	1.59	C18 H32 O16	504.16898	495093920.7	1.079
Coumarin	23.35	C9 H6 O2	146.03668	493676838.5	1.076
Narirutin	25.20	C27 H32 O14	580.17893	435270855.9	0.949
p-Coumaric acid	25.32	C9 H8 O3	164.04725	418489539.4	0.912
Platycodin D	28.30	C57 H92 O28	1224.57522	397289820.4	0.866
Hesperetin	25.78	C16 H14 O6	302.07833	387562280.8	0.845
Cantharidin	23.20	C10 H12 O4	196.07342	371693474.4	0.81
6-Demethoxytangeretin	33.96	C19 H18 O6	342.11006	364957641.6	0.796
Caffeic acid	21.62	C9 H8 O4	180.04214	361938965.3	0.789
Loganic acid	21.78	C16 H24 O10	376.13667	341831205.3	0.745
Sinensetin	33.88	C20 H20 O7	372.12041	336654420.7	0.734
Trigonelline HCl	1.57	C7 H7 N O2	155.05822	323240154.4	0.705
Gracillin	28.29	C45 H72 O17	884.47557	307345804.1	0.67
Stachyose	1.59	C24 H42 O21	666.22190	287742313.2	0.627
Isosinensetin	32.33	C20 H20 O7	372.12042	282971256	0.617
Maltopentaose	1.61	C30 H52 O26	828.27456	236767939.2	0.516
Adenosine	11.81	C10 H13 N5 O4	267.09531	233294424.9	0.509
5-O-Demethylnobiletin	38.93	C20 H20 O8	388.11562	219767965.7	0.479
α-Linolenic acid	43.02	C18 H30 O2	278.22441	206649118.3	0.451
Cynaroside	24.82	C21 H20 O11	448.10044	191934116.5	0.418
Nicotinic acid	2.91	C6 H5 N O2	123.03201	170226691	0.371
Heterophyllin B	30.81	C40 H58 N8 O8	778.43709	165943730.3	0.362
Lobetyolin	26.47	C20 H28 O8	396.17843	153436312.3	0.335

Shanzhiside	20.88	C16 H24 O11	392.13197	141108324.4	0.308
Epiberberine	28.42	C20 H17 N O4	335.11522	134294431.9	0.293
Loganin	22.94	C17 H26 O10	436.15794	128206036.2	0.28
Sarracenin	24.06	C11 H14 O5	226.08397	127208047	0.277
Protocatechualdehyde	21.94	C7 H6 O3	138.03165	115190369.3	0.251
Morroniside	22.22	C17 H26 O11	406.14739	112676668.9	0.246
Azelaic acid	26.48	C9 H16 O4	188.10491	98001283.23	0.214
Rutin	24.32	C27 H30 O16	610.15346	89215318.74	0.195
Lonicerin	24.62	C27 H30 O15	594.15846	87614541.65	0.191
Polyphyllin VI	36.95	C39 H62 O13	738.41880	83903630.06	0.183
Tuberostemonine	25.43	C22 H33 N O4	375.24068	82857550.64	0.181
5-Hydroxymethylfurfural	23.21	C6 H6 O3	126.03166	80784223.09	0.176
Didymin	28.24	C28 H34 O14	594.19451	79729519.79	0.174
Hyperoside	24.80	C21 H20 O12	464.09547	76007547.79	0.166
7-Methoxycoumarin	22.51	C10 H8 O3	176.04727	72095940.01	0.157
Naringenin chalcone	25.21	C15 H12 O5	272.06795	68642386.38	0.15
Vicenin II	22.87	C27 H30 O15	594.15845	68014178.34	0.148
Limonin	34.43	C26 H30 O8	470.19394	67930523.96	0.148
Polyphyllin I	27.88	C44 H70 O16	900.47160	66040280.99	0.144
Desapioplatycodin D	28.13	C52 H84 O24	1092.53424	64087094.26	0.14
Uridine	5.88	C9 H12 N2 O6	244.06948	62313955.66	0.136
Luteolin	28.87	C15 H10 O6	286.04756	58688305.08	0.128
Timosaponin A-III	28.40	C39 H64 O13	740.43382	56335405.07	0.123
p-Hydroxybenzaldehyde	23.58	C7 H6 O2	122.03667	55222706.32	0.12
Sibiricose A5	22.25	C22 H30 O14	518.16355	53896225.31	0.118
Quillaic acid	30.85	C30 H46 O5	486.33425	53798781.6	0.117
Schisandrin	36.41	C24 H32 O7	432.21461	47059009.72	0.103
Vicenin III	23.53	C26 H28 O14	564.14807	43075839.86	0.094

Schisandrin B	46.23	C23 H28 O6	400.18860	42006053.49	0.092
Chrysosplenetin B	35.82	C19 H18 O8	374.10000	41534956.11	0.091
Ruscogenin	36.96	C27 H42 O4	430.30815	40016885.13	0.087
Diosmin	25.68	C28 H32 O15	608.17391	36208751.21	0.079
Oleanonic acid	29.83	C30 H46 O3	454.34458	35179838.23	0.077
Palmatine	28.15	C21 H21 N O4	351.14641	35035414.9	0.076
4-Methyl-6,7-dihydroxycoumarin	22.29	C10 H8 O4	192.04217	32151536.38	0.07
Xanthoxyline	21.77	C10 H12 O4	196.07346	31828456.14	0.069
Abscisic acid	28.40	C15 H20 O4	264.13584	30185430.46	0.066
Isoacteoside	24.56	C29 H36 O15	624.20558	30167087.23	0.066
Diosgenin glucoside	31.26	C33 H52 O8	576.36578	30006996.47	0.065
Isosakuranetin	28.23	C16 H14 O5	286.08360	29840699.5	0.065
Diosmetin-7-O-β-D-glucopyranoside	26.13	C22 H22 O11	462.11599	27188577.44	0.059
Cinnamic acid	24.06	C9 H8 O2	148.05243	25588576.23	0.056
Schizandrin A	45.42	C24 H32 O6	416.21987	22938915.1	0.05
Quercetin	24.81	C15 H10 O7	302.04238	22039908.2	0.048
Diammonium glycyrrhizinate	33.04	C42 H62 O16	822.40380	21815747.04	0.048
Gardenin B	32.20	C19 H18 O7	358.10495	20725171.23	0.045
Cytosine	3.01	C4 H5 N3 O	111.04318	20559691.27	0.045
Apigenin-7-O-β-D-glucoside	25.88	C21 H20 O10	432.10536	20411023.62	0.044
Glabrolide	26.28	C30 H44 O4	468.32381	19533931.76	0.043
Purpureaside C	22.95	C35 H46 O20	786.25831	18995334.84	0.041
Morin	24.34	C15 H10 O7	302.04238	17398581.35	0.038
4-Hydroxybenzoic acid	27.04	C7 H6 O3	138.03164	17051834.94	0.037
Esculetin	23.14	C9 H6 O4	178.02656	16522471.75	0.036

(+)-Magnoflorine	23.37	C20 H23 N O4	341.16246	16296554.62	0.036
Eriocitrin	24.22	C27 H32 O15	596.17402	16092131.66	0.035
2-Hydroxy-4-methoxybenzaldehyde	24.64	C8 H8 O3	152.04727	15996127.51	0.035
Formononetin	32.99	C16 H12 O4	268.07339	15238818.21	0.033
Naringenin	30.69	C15 H12 O5	272.06822	15039633.25	0.033
Kaempferol-3-O-rutinoside	25.11	C27 H30 O15	594.15845	15004527.64	0.033
Rhoifolin	25.52	C27 H30 O14	578.16373	13758008.93	0.03
Ursonic acid	29.48	C30 H46 O3	454.34458	13362150.42	0.029
Obacunone	37.79	C26 H30 O7	454.19911	13107041.01	0.029
Eupatilin	35.21	C18 H16 O7	344.08940	12445179.69	0.027
Baicalin	27.16	C21 H18 O11	446.08472	12295100.53	0.027
Gallic acid	8.20	C7 H6 O5	170.02150	11632984.69	0.025
Orcinol gentiobioside	22.22	C19 H28 O12	448.15800	11144338.23	0.024
Sarsasapogenin	41.06	C27 H44 O3	416.32877	9192027.11	0.02
Diosgenin	40.50	C27 H42 O3	414.31331	8947020.257	0.02
Jatrorrhizine	26.53	C20 H19 N O4	337.13112	8721740.159	0.019
Astilbin	24.71	C21 H22 O11	450.11632	8507454.057	0.019
Calycosin	28.95	C16 H12 O5	284.06816	7367309.65	0.016
Abietic Acid	44.49	C20 H30 O2	302.22444	6966073.332	0.015
Hydroxygenkwanin	31.24	C16 H12 O6	300.06311	6173870.338	0.013
Paeoniflorin	26.26	C23 H28 O11	480.16294	5705709.758	0.012
Rehmannioside D	20.78	C27 H42 O20	732.23292	5642235.036	0.012
Schizandrol B	42.65	C28 H34 O9	531.24700	5609326.168	0.012
Hispidulin	30.66	C16 H12 O6	300.06311	4943780.084	0.011
Spiculisporic acid	39.08	C17 H28 O6	328.18849	4942157.339	0.011
Liguiritigenin-7-O-β-D-apiosyl-4'-O-	24.52	C26 H30 O13	550.16884	4625414.855	0.01

β-D-glucoside					
Apigenin	30.78	C15 H10 O5	270.05255	4154370.16	0.009
Styraxlignolide F	27.96	C27 H34 O11	551.23638	4088322.68	0.009
Pectolinarigenin	33.76	C17 H14 O6	314.07874	3819915.322	0.008
Clareolide	33.55	C16 H26 O2	250.19308	3714868.782	0.008
Oroxylin A-7-O-	29.16	C22 H20 O11	460.10063	3489477.416	0.008
β-D-glucuronide					
Lcaritin	36.25	C21 H20 O6	368.12579	3406843.702	0.007
Ononin	27.18	C22 H22 O9	476.13182	2587203.774	0.006
Cholic acid	35.16	C24 H40 O5	408.28758	2237579.621	0.005

Table S3 Bioactive components of BWBDS.

Components	**Degree**
Sibiricoside A_qt	15
Methylprotodioscin_qt	20
Diosgenin	20
(+)-Syringaresinol-O-beta-D-glucoside	20
4',5-Dihydroxyflavone	11
Beta-sitosterol	68
3'-Methoxydaidzein	14
Sitosterol	22
Baicalein	41
DFV	20
(2R)-7-hydroxy-2-(4-hydroxyphenyl) chroman-4-one	20
4,5'-Retro-.beta.,.beta.-Carotene-3,3'-dione, 4',5'-didehydro-	124
Chryseriol	18
Eriodyctiol (flavanone)	16
XYLOSTOSIDINE	19
Quercetin	147
7-epi-Vogeloside	18

Phytofluene	32
Beta-carotene	58
Secologanic dibutylacetal_qt	4
Centauroside_qt	20
Ethyl linolenate	26
Luteolin	61
Kaempferol	57
Ioniceracetalides B_qt	28
Stigmasterol	30
ZINC03978781	21
Mandenol	11
5-hydroxy-7-methoxy-2-(3,4,5-trimethoxyphenyl) chromone	20
Kryptoxanthin	16
(-) - (3R,8S,9R,9aS,10aS)-9-ethenyl-8-(beta-D-glucopyranosyloxy)-2,3,9,9a,10,10a-hexahydro-5-oxo-5H,8H-pyrano[4,3-d]oxazolo[3,2-a] pyridine-3-carboxylic acid_qt	3
Arachidonate	121
Aposiopolamine	9
Dianthramine	61
Frutinone A	17
Panaxadiol	12
Alexandrin_qt	8
Chrysanthemaxanthin	4
Deoxyharringtonine	17
Diop	35
Inermin	13
Suchilactone	21
Fumarine	6
Girinimbin	12

Ginsenoside Rg5_qt	19
Malkangunin	21
Ginsenoside rh2	29
Gomisin B	10
2-O-methyl-3—O-β-D-glucopyranosyl platycogenate A	18
Robinin	19
Spinasterol	24
Dimethyl 2-O-methyl-3-O-a-D-glucopyranosyl platycogenate A	19
Acacetin	34
Cis-Dihydroquercetin	8
(6Z,10E,14E,18E)-2,6,10,15,19,23-hexamethyltetracosa-2,6,10,14,18,22-hexaene	33
11,14-eicosadienoic acid	91
Mairin	32
Glycyrol	25
(+)-catechin	48
Machiline	16
Glabridin	26
l-SPD	27
CLR	44
Phaseol	12
Estrone	94
Liquiritin	6
Licochalcone B	16
Gondoic acid	75
Isopimaric acid	79
3-Demethylcolchicine	6
Nobiletin	30
Citromitin	5

Naringenin	40
5,7-dihydroxy-2-(3-hydroxy-4-methoxyphenyl) chroman-4-one	29

266